ABSTRACT

Title of Thesis: GEL FORMATION BY THE SELF-ASSEMBLY OF SMALL MOLECULES: INSIGHTS FROM SOLUBILITY PARAMETERS

Kevin Diehn, Master of Science, 2014

Directed by: Prof. Srinivasa R. Raghavan
Department of Chemical & Biomolecular Engineering

Many small molecules can self-assemble into long fibers and thereby gel organic liquids. However, no capability exists to predict whether a molecule in a given solvent will form a gel, a thin solution (sol), or an insoluble precipitate. In this thesis, we build a framework for gelation via a common gelator based on Hansen solubility parameters (HSPs). Using HSPs, we construct 3-D plots showing regions of solubility (S), slow gelation (SG), instant gelation (IG), and insolubility (I) for DBS in different solvents. Our central finding is that these regions radiate out as concentric shells. The distance (R_0) from the central sphere quantifies the incompatibility between gelator and solvent. The elastic moduli of the gels increase with R_0, while the time to gelation decreases with R_0. Our approach can be used to design organogels of desired strength and gelation time by judicious choice of a solvent or a blend of solvents.

GEL FORMATION BY THE SELF-ASSEMBLY OF SMALL MOLECULES: INSIGHTS FROM SOLUBILITY PARAMETERS

Kevin K. Diehn

Thesis submitted to the Faculty of the Graduate School of the
University of Maryland, College Park, in partial fulfillment
of the requirements for the degree of
Master of Science
2014

Advisory Committee:

Prof. Srinivasa R. Raghavan, Chair

Prof. Mikhail Anisimov

Prof. Jeffery Klauda

Dedication

This thesis is dedicated to my family, friends, and co-workers,

without whose support this work would have not been possible.

Acknowledgements

I would like to thank my advisor, Dr. Srinivasa Raghavan, who has guided me through my research career to this point. Dr. Raghavan's has consistently offered a positive outlook and support in pursuing my research goals. Moreover, his emphasis on fundamental understanding and clear communication of research results has shaped my abilities as a scientist.

I would also like to thank all of my Complex Fluids group labmates who have offered me support and friendship throughout this work.

I would also like to thank Dr. Richard Weiss of Georgetown University who provided consistent encouragement and vision for the potential of this work.

TABLE OF CONTENTS

Chapter 1: Introduction and Overview

Molecular organogels are a fascinating class of materials that are attracting wide interest among chemists, physicists and engineers.[1-3] They are formed by the non-covalent self-assembly of small molecules in organic liquids. The molecular assembly results in long one-dimensional objects ("fibers"), which entangle and interconnect into a three-dimensional (3-D) network.[4] Upon formation of such a self-assembled fibrous network (SAFIN), the liquid solvent (sol) is entrapped within the network, and the sample is transformed into an elastic gel (Figure 1.1). Molecular organogels are being explored for a variety of applications such as for treating oil spills,[5] art conservation,[6] plasma and serum separation,[7] and as materials in solar cells or lithium-ion batteries[8].

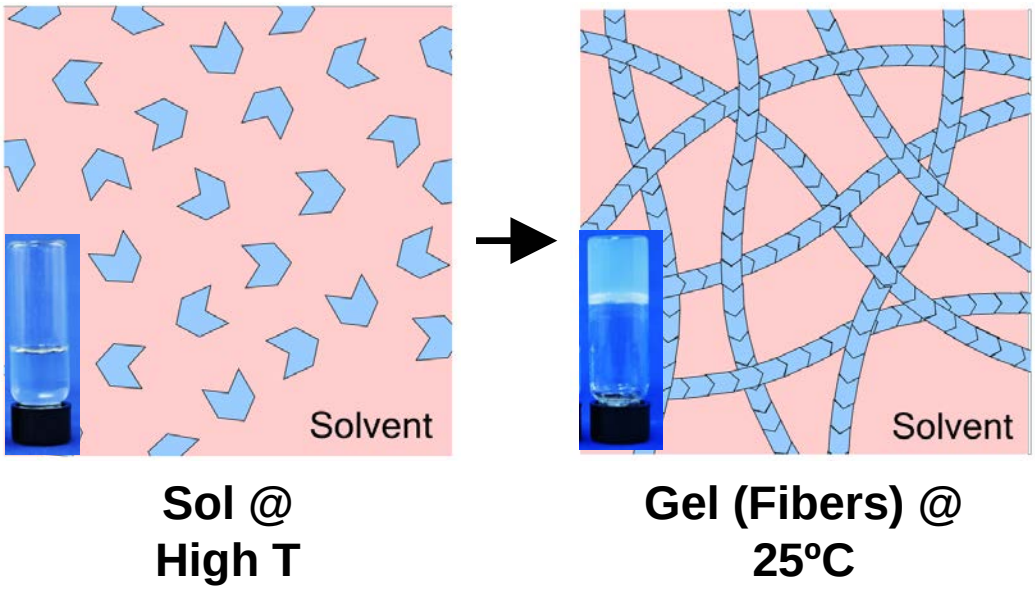

Figure 1.1. Schematic of Small Molecule Self-assembly into Fibers and Gels. At high temperature (left) gelator molecules (blue arrows) are discrete entities and the sample is a sol (solution). As the sample is cooled to room temperature (right), the molecules assemble into long fibers that entangle to entrap the solvent and form a gel.

Despite the wide interest in molecular gels, a fundamental understanding of self-assembly-based gelation is lacking. Most known organogelators have been discovered by serendipity, and trial-and-error experiments are still necessary to determine which solvents they can gel.[2,9,10] It would be invaluable to have a framework that could be used to predict whether a given gelator could gel a new solvent of interest. For various solvents, important physical properties such as the dielectric constant, Hamaker constant, surface tension, Hildebrandt solubility parameter, and Hansen solubility parameters, are either tabulated or can be calculated. Can gelation be correlated with one or more of these physical properties? This question has generated much research,[11-15] but the field still awaits a framework that has applicability across a wide range of molecular gelators.

An important advance in connecting gelation with solvent properties was recently reported by Raynal and Bouteiller[16] who performed a meta-analysis of eight earlier studies on organogelators. They interpreted these results in terms of the solvents' Hansen solubility parameters (HSPs).[17,18] HSPs quantify the cohesive energy density δ of a solvent in terms of contributions from three types of weak interactions:[17] van der Waals or dispersive interactions (δ_D), dipole-dipole or polar interactions (δ_P), and hydrogen-bonding interactions (δ_H). Each solvent is thus a point on a 3-D plot in which the axes represent the three HSPs (δ_D, δ_P, and δ_H). The distance from the origin to that point represents the total cohesive energy density δ of the solvent.[17] The same approach has also been subsequently used by other researchers.[19-23] In this thesis, we develop a new HSP-based framework for interpreting gelation that offers important insights and useful predictive capabilities.

The focus of our studies is the well-known model organogelator 1,3:2,4-dibenzylidene sorbitol (DBS). DBS is a butterfly-shaped molecule with a hydroxylated center and benzyl groups on either side (Figure 1.2) and it is capable of gelling many organic solvents at low concentrations (< 5 wt%).[21,24-31] We examine DBS in a wide range of solvents with known HSPs and we plot our observations on 3-D Hansen plots. (Note that the precise HSPs of DBS are not known *a priori*. Group contribution methods do exist to determine HSPs from the functional groups present in a given molecule;[17, 21] however, these can be reliably applied only to simple molecules, not to complex structures like DBS.) Our central finding is a consistent, logical progression in 3-D Hansen space with spherical shells of solubility, gelation, and insolubility radiating out in order (see Chapter 3). This pattern offers insights into both the nature and the kinetics of gelation. In addition, we are also able to correlate the rheology of DBS gels with the solvent properties based on HSPs.

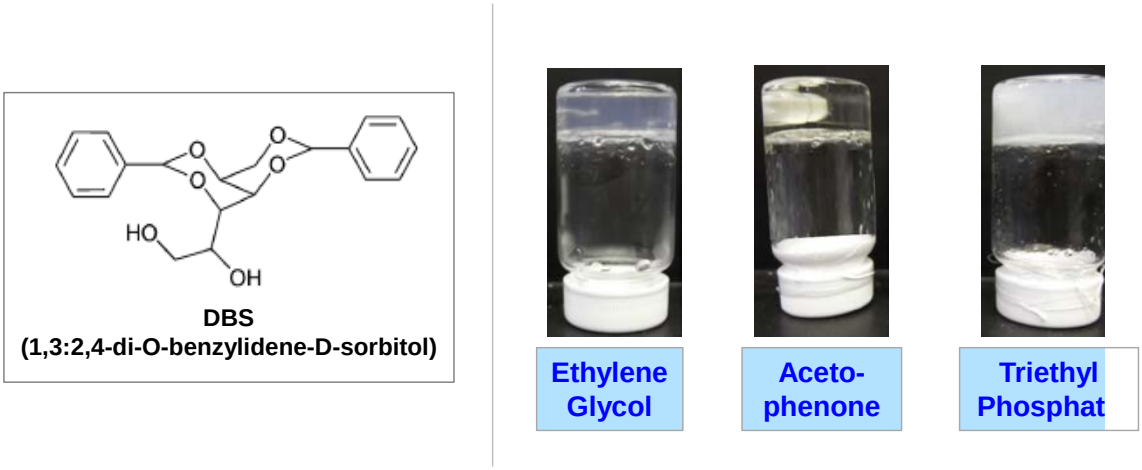

Figure 1.2. Structure of DBS and Photographs of DBS Gels. (Left) The butterfly-like structure of DBS is shown. (Right) Gels of DBS in various solvents is shown.

The significance of this work lies in the framework we have advanced for characterizing the self-assembly of organogelators in different solvents. Our work suggests that gelation requires a moderate extent of incompatibility between the gelator

and solvent. Our approach gives reasonable predictions of gelator behavior in untested solvents, such as solvent blends. Some thumb rules based on our approach have been developed, and we hope these will be tested by experiments with other gelators. A MATLAB program and an associated graphical user interface (GUI) have been developed to allow other researchers to apply the same approach to other gelators.

Chapter 2: BACKGROUND

In Chapter 2, we provide background on each of the key components of our study. Molecular organogels are the focus of our study and we have studied a particular gelator, 1:3,2:4-dibenzylidene sorbitol (DBS), as a model gelator. We have characterized the behavior of DBS in a variety of solvents, whose properties can be quantified by Hansen Solubility Parameters (HSPs). An introduction to HSPs is provided and their utility is discussed. Finally, we have characterized our gels via rheology, and we provide a basic background into rheological techniques.

2.1. MOLECULAR ORGANOGELS

Molecular organogels are a class of soft materials consisting of an organic solvent entrapped in a self-assembled fibrous network (SAFIN). The SAFIN is formed via the self-assembly of a small molecule, which is referred to as low-molecular weight organogelator (LMOG). To form an organogel, the LMOG is dissolved to form a transparent solution (sol) by heating. When this sol is cooled, the gelator molecules interact with one another via weak bonds (Van der Waals interactions, hydrogen bonds, π-π bonds etc.) to form long, one-dimensional fibrillar structures. As these fibrils grow, they entangle into a three-dimensional network that immobilizes solvent molecules to form a gel. The formation of the gel may be reversed by heating the gel to break the weak interactions between the LMOG molecules within each fibril.[1-3]

As mentioned, gelator molecules have drawn significant interest in the past two decades for their vast commercial potential.[5-8] However, a major limitation currently is in determining *a priori* if a gelator will gel a given solvent. Currently, such predictive capability does not exist and researchers have to perform numerous tests in different solvents with each gelator that is synthesized or discovered.

2.2. ORGANOGELS MADE FROM DBS

In this work, we have chosen 1:3,2:4-dibenzylidene sorbitol (DBS) as a model organogelator. DBS is a small, butterfly-shaped sorbitol derived molecule with a hydroxyl center and benzyl groups on either side (Figure 1.2) that is capable of assembling into long fibrils and thereby gelling a variety of organic solvents at low concentrations (in many cases at < 1%). DBS has been widely studied[21,24-31] and even found industrial applications in the gelation of cosmetics products.[32] Despite the numerous studies on DBS, little is understood about DBS self-assembly. The primary driving force for the self-assembly of DBS appears to be a combination of hydrogen bonding and π-π bonds, although the exact mechanism by which DBS self-assembles into fibrils remains largely unknown.

Remarkably, the behavior of DBS varies widely from solvent to solvent. DBS is readily soluble in some solvents, such as n-methylpyrrolidone (NMP) and dimethylformamide (DMF), yet DBS is a potent gelator of glycols, silicone fluids, alcohols, and aromatics. In other solvents, such as non-polar aliphatics or water, DBS remains completely insoluble even at high temperature. Moreover, even among solvents gelled by DBS, the properties of the final gels vary widely. In some solvents

DBS forms a transparent gel, while in others the gel appears highly opaque (see Figure 1.2). Some gels are very soft (low modulus), while others are very stiff (high modulus). Likewise, as we will discuss, even the kinetics of DBS gelation (i.e., how quickly the gel forms after the sol is cooled to room temperature) varies widely from a few seconds to days or weeks depending upon the choice of solvent. Up to this point, no conclusive studies exist to tie the highly varied behavior of DBS across solvents together into a simple framework.

2.3. HANSEN SOLUBILITY PARAMETERS

Hansen solubility parameters (HSPs) are a means to quantify the non-covalent interactions between molecules of a given solvent.[17,18] The parameters are an extension of the Hildebrand solubility parameters, which have been commonly used by polymer scientists for predictive estimates of polymer solubility in solvents. The basis for Hildebrand solubility parameters is that the cohesive energy between molecules of a given solvent determines how likely it is to dissolve a given solute or be miscible with another solvent. The cohesive energy can be easily quantified from the enthalpy of vaporization (E_{vap}) for the solvent. The E_{vap} provides an estimate of how much energy is required to pull molecules apart from a highly interacting state (liquid phase) to a non-interacting state (vapor phase). While Hildebrand parameters are effective for predicting behavior of relatively non-polar species in non-polar solvents, they are limited for prediction of systems with significant polarity or hydrogen bonding effects. To overcome this limitation, HSPs quantify the cohesive energy density δ of a solvent in terms of contributions from three types of weak interactions: van der Waals or

dispersive interactions (δ_D), dipole-dipole or polar interactions (δ_P), and hydrogen-bonding interactions (δ_H). Thus, each solvent has three HSPs assigned to it. Parameters for hundreds of solvents have been empirically determined and tabulated by Hansen in his book.[17] Using these known HSP values for different solvents, it is possible to test an unknown solute (typically a polymer) in these solvents, plot the results in 3-D space (Figure 3.1; as described below), and thus predict the solubility of the solute in untested solvents.

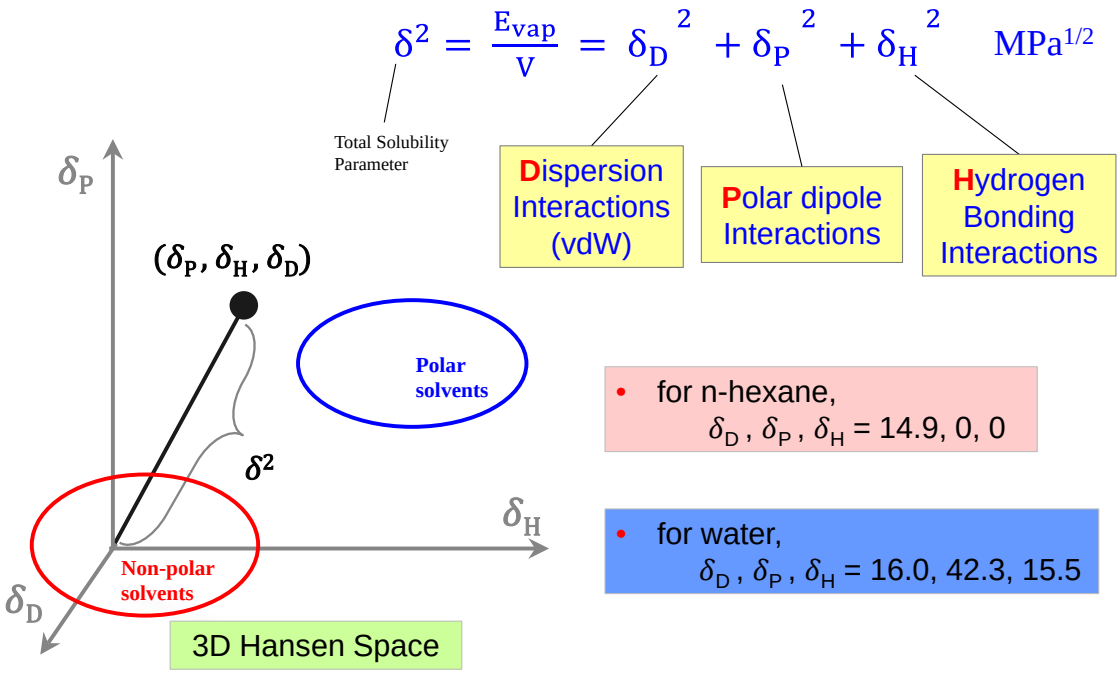

Figure 2.1 Schematic of Hansen Solubility Parameters and 3-D Hansen Space.

Based on the three HSPs, one may construct a 3-D Hansen space in which each solvent is represented as a single point and the distance from the origin to the point represents the total cohesive energy density (δ) of the solvent (Figure 3.1). On this plot, non-polar solvents exist mainly near the origin, while highly polar solvents are far from the origin. For example, *n*-hexane has co-ordinates (δ_D, δ_P, δ_H = 14.9, 0, 0), which means it falls very near the origin. In comparison, water is the farthest solvent from the origin (δ_D, δ_P, δ_H = 16.0, 42.3, 15.5). The essential idea of using this plot for solubility analysis is that *a solute is likely to have greater solubility in a solvent that is close to its coordinates* in 3-D Hansen space. Furthermore, for a given solute, Hansen's work suggests that a sphere can be drawn around the solute's 3-D coordinates that will encompass the solvents in which it is soluble ("good" solvents) and exclude the solvents in which it is not ("bad" solvents).

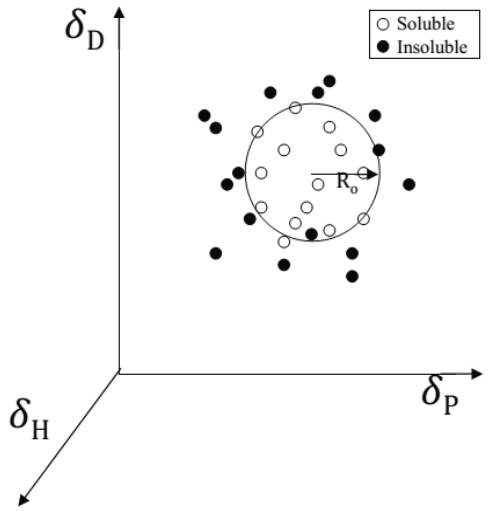

Figure 2.2 Schematic of a solubility sphere for a solute in 3-D Hansen Space. The "good" solvents are indicated by open circles and the "bad" solvents by filled circles. The solubility sphere encompasses the good solvents while excluding the bad ones.

In addition to empirical values for solvent HSPs, Hansen's book provides a simple method to determine a solubility sphere (Figure 3.2) for a given solute at a given temperature and pressure. First, a solute (typically a polymer) of unknown solubility and HSPs is tested for solubility in a variety of solvents of known HSPs at a given temperature and pressure. Then, the "soluble" or "insoluble" data points are plotted in 3D Hansen space. Next, a good guess for the center of the solubility sphere is made either by averaging the soluble points or by inspection. Finally, a sphere of radius R_0 is drawn such as to include as many of the "soluble" points as possible inside the sphere and exclude as many of the "insoluble" points as possible outside the sphere (Figure 3.2). This fitting process may be performed roughly by inspection or more precisely through iterations of a "goodness of fit" equation (see Chapter 3).

2.4. RHEOLOGY

Rheology is defined as the study of a material's flow and deformation under stress. It is of great importance in the characterization of polymers and soft materials such as molecular gels. In particular, rheology is very useful for measuring the physical properties of *viscoelastic* materials, which contain both liquid-like *viscous* characteristics and solid-like *elastic* characteristics. In this study, we have utilized parallel plate rheology in which the sample is loaded onto a stationary bottom plate with a Peltier attachment to control temperature. After loading the sample, a top plate is lowered to the sample and rotates (or oscillates) to apply a stress on the sample. Rheological characterization is generally performed under two conditions: 1) steady shear rheology, in which the top plate shears the sample at a constant strain rate, or 2)

dynamic (or oscillatory) shear rheology, in which the top plate oscillates at a fixed strain at various frequencies. In our study, oscillatory rheology was used to measure the gel modulus to compare the properties of DBS gels in various solvents.

In a dynamic rheology measurement, the top plate applies a sinusoidal strain $\gamma = \gamma_0 \sin(\omega t)$ to the sample, where γ_0 is the maximum amplitude of the strain and ω is the frequency. The response of the sample will be a sinusoidal stress, $\sigma = \sigma_0 \sin(\omega t + \delta)$, where σ_0 is the stress amplitude and δ is the phase shift relative to the strain waveform. Using trigonometric identities, the stress response of the material can be decomposed into two components as follows:

$$\sigma = G'\gamma_0 \sin(\omega t) + G''\gamma_0 \cos(\omega t) \tag{2.1}$$

In this equation, G' represents the *solid-like* or *elastic* modulus and G'' represents the *liquid-like* or *viscous* modulus of the material. In order for these values to be a true representation of a material's properties, the measurements must be taken in the *linear viscoelastic regime* of the material, such that the elastic and viscous moduli are solely functions of frequency. Finally, in the case of an elastic or gel-like material, the value of G' is approximately constant across all frequencies (i.e., the gel does not relax over all timescales). The constant value of G' quantifies the *stiffness* of the material.

Chapter 3: INSIGHTS INTO DBS ORGANOGELATION VIA HANSEN SOLUBILITY PARAMETERS

3.1. INTRODUCTION

In this chapter, we demonstrate a new framework in which we apply Hansen Solubility Parameters (HSPs) to characterize the varied outcomes of a model gelator. To do this, we study the behavior of our model organogelator, DBS, in 34 organic solvents at three DBS concentrations and at room temperature. The sample outcomes vary greatly from solvent to solvent, and in this work, we have classified the outcomes into one of four classes: soluble, slow gel, instant gel, or insoluble. For each solvent we have access to the three HSP values, as discussed in Chapter 2.3.[17] Based on these parameters, we plot each sample in 3-D Hansen space. Then, using an algorithm proposed by Hansen for determining polymer solubility, we fit the data with spheres around each point via MATLAB. We find that the behavior of DBS in 3-D Hansen space is fit well by concentric spheres radiating out from a central solubility sphere. Likewise, we have correlated gel modulus and time of gelation with distance from the center of the central solubility sphere.

An additional aspect of our work is in the mapping and prediction of DBS behavior in *blends* of solvents. Herein, we have collected data on DBS sample outcomes in various mixtures of solvents. Remarkably, while complexity of solvent mixtures would suggest that prediction of gelator behavior would be quite difficult, our results are promising. Though the size of the soluble, slow gel, instant gel, and insoluble regions changes, generally, we have found that the *trends* observed in neat

solvents remains the same. For example, mixtures of a solvent that solubilizes DBS and a solvent in which DBS is insoluble will produce samples which show an expected transition from soluble to slow gel to instant gel to and insoluble as the composition of the mixture shifts. A recent study showed that a gelator could be combined with two neat solvents in which it is insoluble and that it would form a gel in mixtures of these solvents. Similarly, our results predict that nitromethane and octanol, in which DBS is initially insoluble, would show the three other DBS outcomes (soluble, slow gel, instant gel) in their mixtures.

In the process of this study, we have implemented our HSP fitting algorithm via MATLAB and generated a graphical user interface (GUI) for obtaining 3-D plots of the sample outcomes and the corresponding spherical fits. This program will be available upon request to other researchers, as it is our hope that the the methods presented in this thesis will facilitate greater understanding of all types of organogelator behavior.

3.2. EXPERIMENTAL SECTION

Materials

DBS (1,3:2,4-divinylbenzylidene sorbitol) was obtained from Milliken Chemicals. All solvents were acquired from Sigma-Aldrich and TCI America and used without further purification.

Preparation of DBS Gels

DBS powder was added to solvents at desired weight-by-volume percent. Samples were heated to 125°C until a transparent sol was obtained. (Note that for volatile samples with a boiling point near to or less than 125°C, special high- pressure capable vials were used to ensure that no sample evaporation occurred.) If samples could not be dissolved, they were classified as insoluble. Samples were cooled with running water (22°C) for 90 seconds until they reached room temperature. They were then placed on the countertop for further observation. The classification scheme is further described in the main text.

Rheological Studies

Dynamic rheological experiments were performed on an AR2000 stress-controlled rheometer (TA Instruments). Samples were run on a parallel-plate geometry (25 mm plate, 0.5 mm gap). Dynamic frequency spectra were obtained in the linear viscoelastic regime of each sample, as determined by dynamic strain-sweep experiments.

Description of Fitting Procedures and Algorithm

In order to visualize the regions of DBS outcomes, each solvent point is plotted in 3-D Hansen space, where each axis represents one of the HSPs (δ_D, δ_P, and δ_H). The solvent points are color-coded based on the outcome of the sample (Soluble, **S** = blue; Slow Gel, **SG** = green; Instant Gel, **IG** = red; Insoluble, **I** = yellow). Next, spheres are drawn around these regions in 3-D space as prescribed by Hansen for polymer solubility studies. The spheres are defined by their center point ($\delta_{Dcenter}$, $\delta_{Pcenter}$, $\delta_{Hcenter}$) and their radius *R*. To determine the best placement and size of the sphere, the sphere must be drawn such that "good" solvent points lie inside it and "bad" solvent points are excluded from it. We start with the sphere for the sol (**S**) region. In this case, soluble points should be inside the **S** sphere and all other points should be outside. A desirability function is used to determine the goodness-of-fit for a given radius and center point of the sphere. The desirability function (DF) is defined as:

$$\text{Desirability Function (DF)} = \left(A_1 \times A_2 \times \ldots A_n\right)^{\frac{1}{n}}$$

$$\text{where } A_i = \begin{cases} 1 & \text{for good solvent inside sphere} \\ 1 & \text{for bad solvent outside sphere} \\ e^{-\left|R_i - R_S\right|} & \text{for all other cases} \end{cases} \tag{3.1}$$

where R_i is the distance in 3-D Hansen space from the solvent point *i* to the center of the **S** sphere and R_S is the radius of the **S** sphere. *n* is the total number of solvent points. We use an algorithm based on Hansen's work in which the center of the **S** sphere is guessed based upon the soluble points, the optimal value of the radius R_S is determined via value of the DF, and the process is repeated for nearby values of the center point. The initial guess for the center of the **S** sphere is based on the average HSP of each of the solvents in which DBS is soluble. With this initial center point, the radius R_S of this

sphere is varied from very small values ($R_{S,min}$ = 1) to very large values ($R_{S,max}$ = 25). Based on the DF value at each of these radii, the optimal radius is selected.

Next, a cube (usually of side length L = 1) is drawn around the initial guess of the center point. For each corner of the cube, the optimal value of the sphere radius is determined by varying the radius and calculating the value of the DF. From these nine points (eight points at the cube corners and one point in the cube center), the point with the highest value of the DF is selected. If the point with the highest DF is the cube center, the algorithm repeats the cube iteration with a cube of a smaller length (L= 0.5, then L = 0.3) until the best center and radius combination is determined. If the point with the highest DF is one of the cube corners, the cube iteration is repeated. Ultimately, we determine the combination of center point and radius R_S that maximizes the DF. This fixes the solubility **S** sphere.

For the remaining 3 outcomes (**SG**, **IG** and **I**), the center point of the corresponding spheres is fixed to be identical to that of the **S** sphere (see below). The iteration is then done only to optimize the radii of these spheres. It should be noted that our analysis procedure is general enough and can account for each outcome having distinct sphere centers as well as radii. The MATLAB program written for this study (Figure 3.1) allows the user to choose between the two options.

Figure 3.1. Overview of MATLAB HSP 3D Plotting and Fitting Program

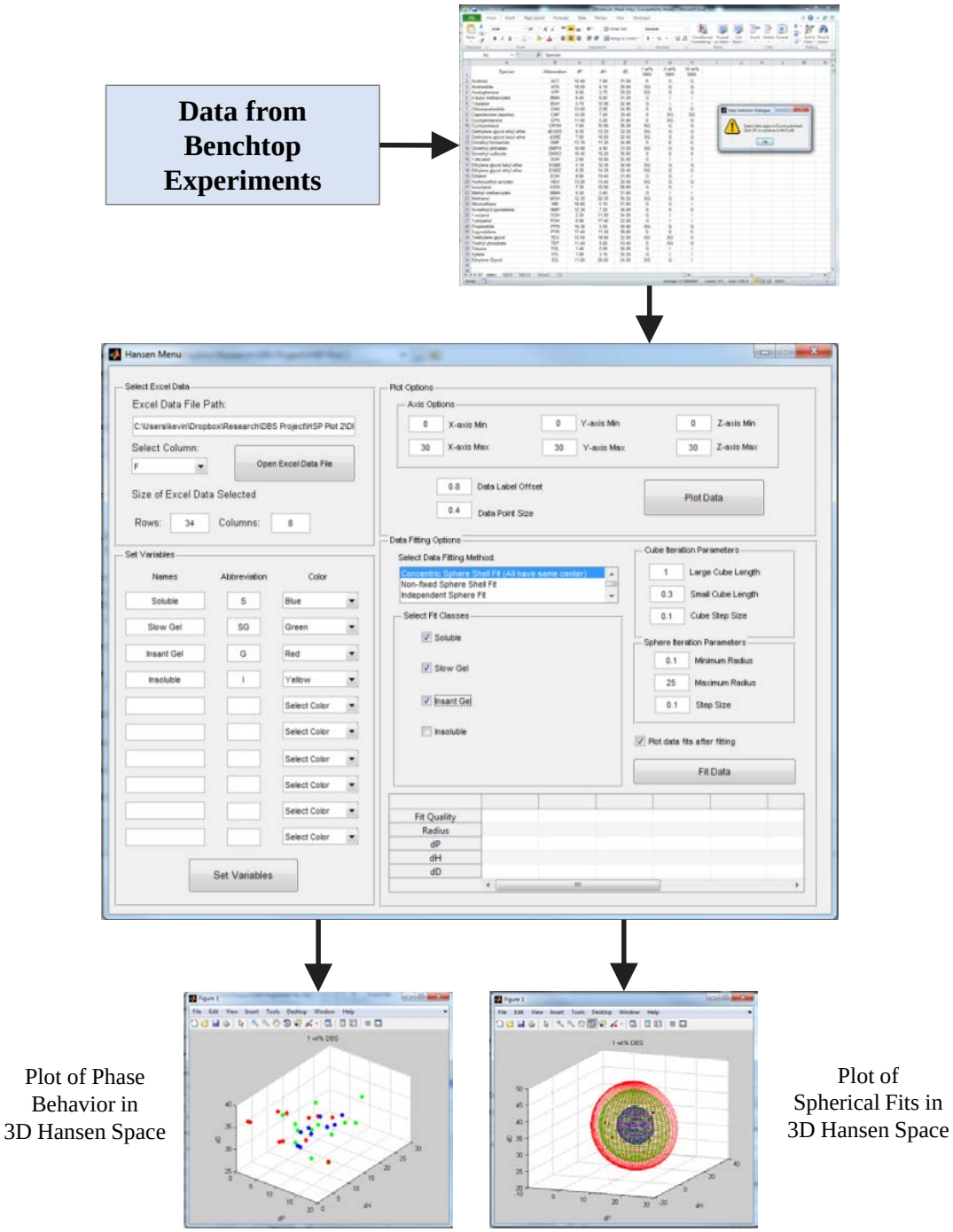

3.3. RESULTS AND DISCUSSION

3.3.1 OBSERVATION AND CLASSIFICATION OF SAMPLE OUTCOMES

The HSPs for hundreds of neat organic solvents are collected in the book by Hansen.[17] We studied DBS in many of these solvents, with some candidate solvents identified from the previous literature.[21, 25-31] Our procedure employed visual observation of DBS-solvent mixtures and is schematically depicted in the top panel of Figure 3.2. First, DBS was added to the solvent at a desired concentration and the mixture was heated to 125°C while being stirred. This typically resulted in a thin, transparent liquid (sol). The vial containing the hot sol was then cooled to room temperature using running water (22°C) for 90s. From this point onwards, the vial was placed on the countertop and observed visually. Vial inversion was used to infer the formation of an organogel, i.e., a sample was termed a gel if it held its own weight in the inverted vial.[33]

Sample outcomes were categorized in the following manner (Table 3.1). A sample was classified to be insoluble (**I**) if: (a) it could not be dissolved after heating and stirring, or (b) it was soluble at high temperature (*T*) but gave a solid precipitate upon cooling to room temperature. Photo 4 in Figure 3.2 is an example of such a sample. Next, a sample was classified as a sol or soluble (**S**) if it remained a thin, clear solution indefinitely after cooling to room temperature (Photo 1). That is, sols remained so regardless of time; they did not subsequently convert into gels or become precipitates. Next, concerning the samples that did transform from sols at high *T* to gels at ambient temperature, we further distinguished two cases depending on the kinetics of the gelation. If the sample was already a gel (as indicated by vial inversion) by the

time it was cooled to room temperature (time $t = 0$), it was classified as an instant gel (**IG**). If the sample was not a gel at $t = 0$ but formed a gel at some finite time t_{gel} after reaching room temperature, it was classified as a slow gel (**SG**) and the corresponding t_{gel} was recorded. The distinction between **IG** and **SG** is important because gelation is a non-equilibrium process and there is a kinetic aspect to it.[2, 34] For example, many gels, including DBS, form by the nucleation and growth of fibrils. Thus, a simple either-or approach could produce different results depending on the procedure and the time at which the sample is observed. The use of the four-pronged **S-SG-IG-I** scheme mitigates against these issues.

Species	Abbr.	δ_P	δ_H	$2\delta_D$	1 wt% DBS	5 wt% DBS	10 wt% DBS
Acetone	ACT	10.40	7.00	31.00	S	IG	IG
Triethyl phosphate	TEP	11.40	9.20	33.40	S	SG	IG
Cyclopentanone	CPN	11.90	5.20	35.80	S	SG	IG
N-methyl-2-pyrrolidone	NMP	12.30	7.20	36.00	S	S	S
Chloroacetonitrile	CAN	13.60	2.00	34.80	S	IG	IG
Dimethyl formamide	DMF	13.70	11.30	34.80	S	S	S
Caprolactone (epsilon)	CAP	15.00	7.40	39.40	S	SG	SG
Dimethyl sulfoxide	DMSO	16.40	10.20	36.80	S	S	S
2-pyrrolidone	PYR	17.40	11.30	38.80	S	S	S
Ethylene glycol butyl ether	EGBE	5.10	12.30	32.00	SG	IG	IG
Diethylene glycol butyl ether	dEGBE	7.00	10.60	32.00	SG	IG	IG
Cyclopentanol	CPOH	7.60	15.60	36.20	SG	IG	IG
Acetophenone	ATP	8.60	3.70	39.20	SG	IG	IG
Diethylene glycol ethyl ether	dEGEE	9.20	12.20	32.20	SG	IG	IG
Ethylene glycol ethyl ether	EGEE	9.20	14.30	32.40	SG	IG	IG
Dimethyl phthalate	DMPH	10.80	4.90	33.20	SG	IG	IG
Ethylene Glycol	EG	11.00	26.00	34.00	SG	IG	I
Methanol	MOH	12.30	22.30	30.20	SG	IG	IG
Triethylene glycol	TEG	12.50	18.60	32.00	SG	SG	IG
Hydroxyethyl acrylate	HEA	13.20	13.40	32.00	SG	IG	IG
Propionitrile	PPN	14.30	5.50	30.60	SG	IG	IG
Acetonitrile	ATN	18.00	6.10	30.60	SG	IG	IG
Xylene	XYL	1.00	3.10	35.20	IG	I	I
Toluene	TOL	1.40	2.00	36.00	IG	I	I
1-decanol	DOH	2.60	10.00	35.00	IG	I	I
1-octanol	OOH	3.30	11.90	34.00	IG	I	I
1-butanol	BOH	5.70	15.90	32.00	IG	I	I
n-butyl methacrylate	BMA	6.40	6.60	31.20	IG	I	I
Methyl methacrylate	MMA	6.50	5.40	31.60	IG	I	I
1-propanol	POH	6.80	17.40	32.00	IG	I	I
Isooctanol	iOOH	7.30	12.90	28.80	IG	IG	I
Ethanol	EOH	8.80	19.40	31.60	IG	IG	I
Nitromethane	NM	18.80	5.10	31.60	IG	IG	I
Decane	DEC	0	0	31.4	I	I	I

Table 3.1. Solvents tested and DBS sample outcomes in these solvents

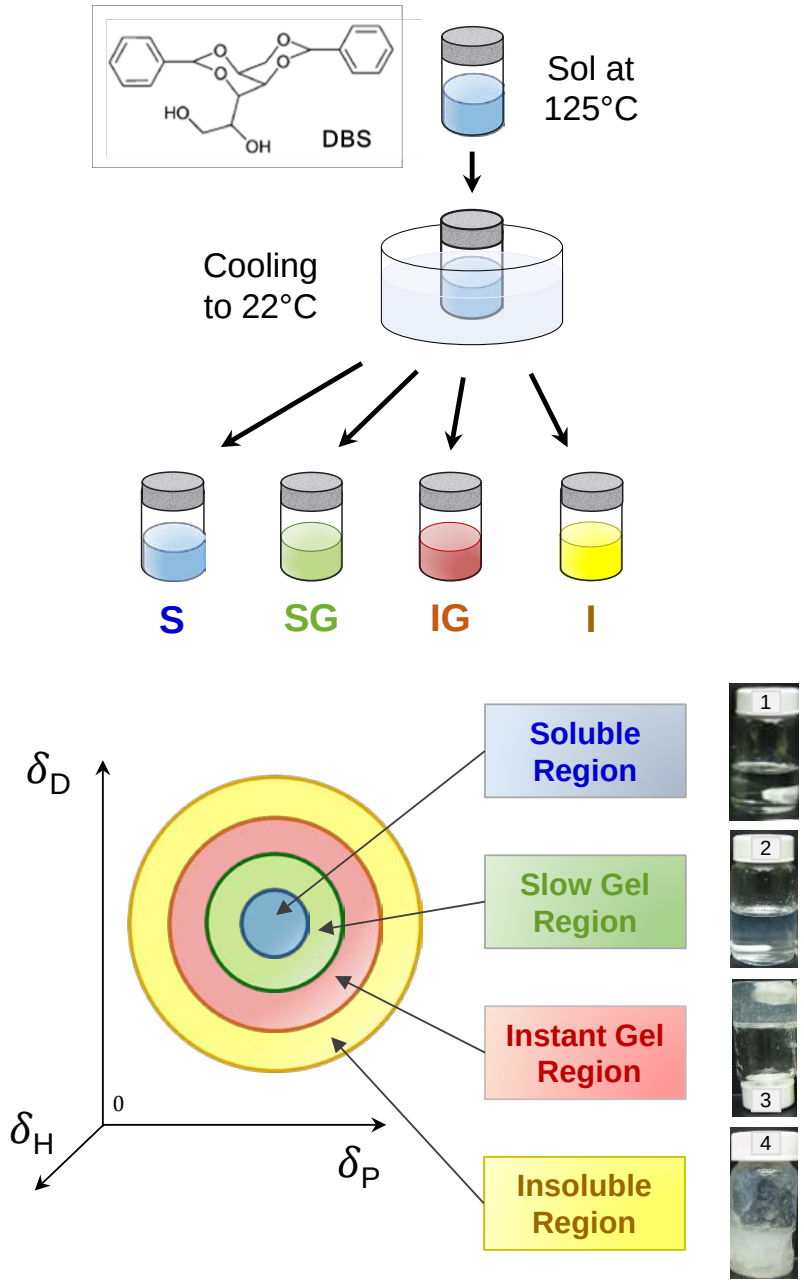

Figure 3.2. Schematic of the experimental setup (top) and the corresponding results in 3-D Hansen space (bottom). DBS was added to various solvents and heated to 125°C, followed by cooling to room temperature (22°C). Visual observations were used to classify the samples as soluble or sols (S, blue), slow gels (SG, green), instant gels (IG, red) and insoluble (I, yellow). Photographs of samples corresponding to these outcomes are shown. These outcomes were then plotted for the solvents on a 3-D plot where the axes are the three Hansen solubility parameters (D = dispersive, P = polar, and H = hydrogen-bonding interactions). Our key finding, shown by the schematic is that the four regions radiate out as concentric shells: i.e., a central sol (S) sphere, followed in order by SG, IG, and I spheres.

3.3.2 PLOTTING OUTCOMES IN 3-D HANSEN SPACE

To visualize the regions of DBS outcomes, each solvent was plotted as a point in 3-D Hansen space where each axis represents one of the HSPs (δ_D, δ_P, and δ_H). The solvent points were color-coded based on the outcome of the sample, with blue for soluble (**S**), green for slow gel (**SG**), red for instant gel (**IG**), and yellow for insoluble (**I**). Next, color-coded spheres were drawn around each of these regions on the 3-D plot. The use of spherical regions mirrors the method used by Hansen for polymer-solvent interactions.[17, 18] In our approach, we have made a few critical choices that departs from previous work on HSP-gelator correlations. First, we begin by focusing on the blue sphere corresponding to the soluble (**S**) region in Figure 3.2. The criterion for this sphere is that it must encompass all the solvents in which DBS gives a sol (the "good" solvents) while excluding all other solvents (the "bad" solvents). The size of the **S** sphere (i.e., its radius R_S) and its location (i.e., its origin in 3-D space) are the two variables. We used a MATLAB program (Figure 3.1) to find the location and size of the optimal **S** sphere that satisfied the above criterion. As discussed, we make an initial guess for the location of the origin and an initial value of the radius based on our data. Taking cues from Hansen's work, we employ a desirability function (DF, eq 3.1) to determine the goodness-of-fit for this radius and origin.[17, 18] We then iterate the location and size of the **S** sphere until the DF is maximized.

Once the soluble (**S**) sphere is correctly sized and placed, *we then use the same origin for the subsequent **SG**, **IG** and **I** spheres*. This is a crucial distinction from previous studies and we believe it leads to a simpler and more intuitive framework. The resulting plots are shown schematically in Figure 3.2. Considering the **SG** (green)

sphere, we fix its origin as that of the **S** (blue) sphere and iterate its radius R_{SG} such that it encompasses the solvents in which DBS forms a slow gel while excluding the solvents corresponding to the **IG** and **I** outcomes. Similarly, we draw the **IG** (red) sphere under the criterion that it includes the solvents in which DBS forms an instant gel while excluding the solvents in which DBS is insoluble. Finally, we plot the **I** (yellow) sphere by extending it up to the solvent points corresponding to DBS insolubility. Our central result is that the four regions radiate out as concentric shells (Figure 3.2): i.e., the central soluble (**S**) sphere is followed in order by spheres corresponding to the **SG**, **IG**, and **I** regions. We will discuss the implications of this result after first presenting the actual data.

3.3.3 3-D SOLUBILITY PLOTS FOR DBS

DBS sample outcomes were determined and plotted by the above procedure for three DBS concentrations: 1%, 5% and 10% (weight/volume). A total of 34 solvents were tested and their HSPs are provided in Table 3.1. The plots in 3-D Hansen space are shown in Figure 3.3. Note also that these results pertain to room temperature (~ 22°C). For convenient representation, the vertical axis is not extended to the origin and its values correspond to $2\delta_D$; the other two axes correspond to δ_P, and δ_H. The use of $2\delta_D$ is per the recommendation of Hansen as it is conducive to spherical fits.[17,18]

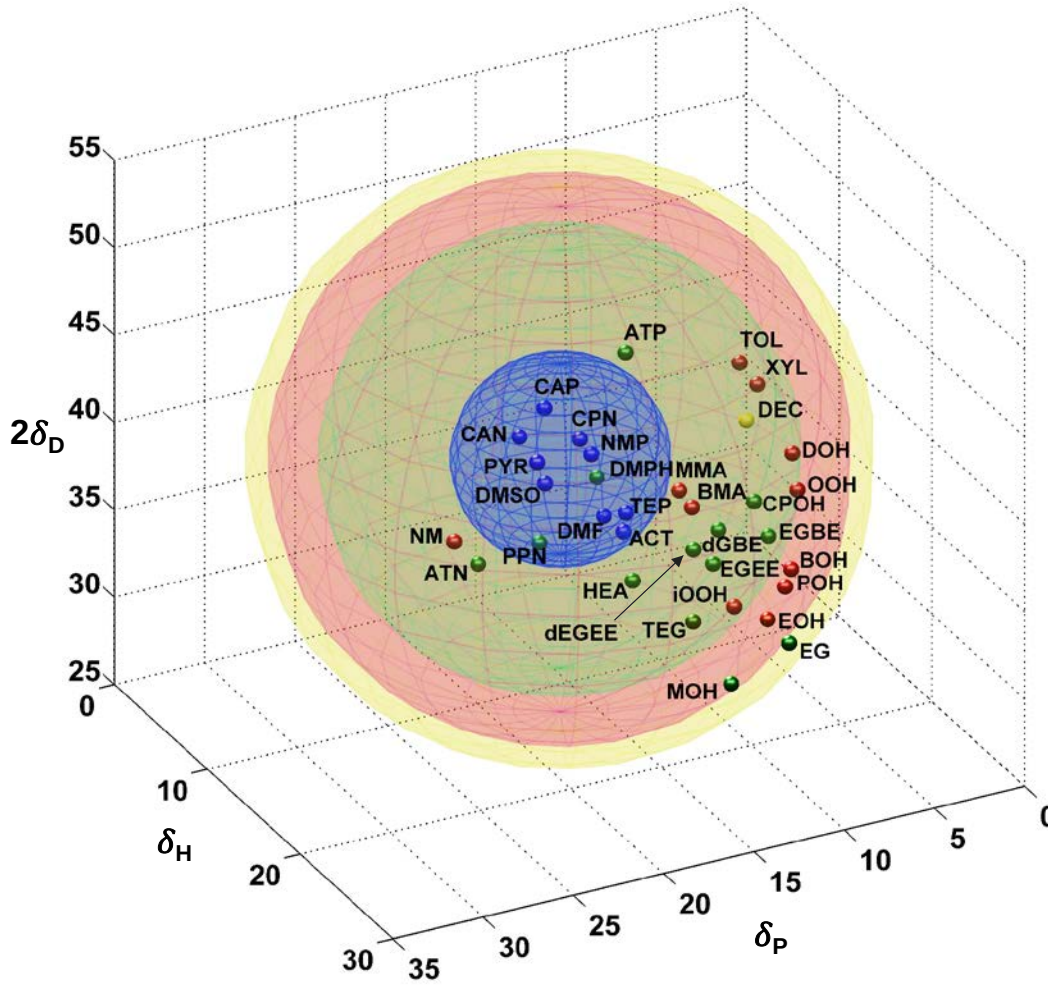

(a) 1% DBS

Sol (S) Center:

$(\delta_P, \delta_H, 2\delta_D) =$

$(13.6, 6.4, 35.6)$

$R_S = 5.5$

$R_{SG} = 12.0$

$R_{IG} = 14.5$

$R_I = 15.6$

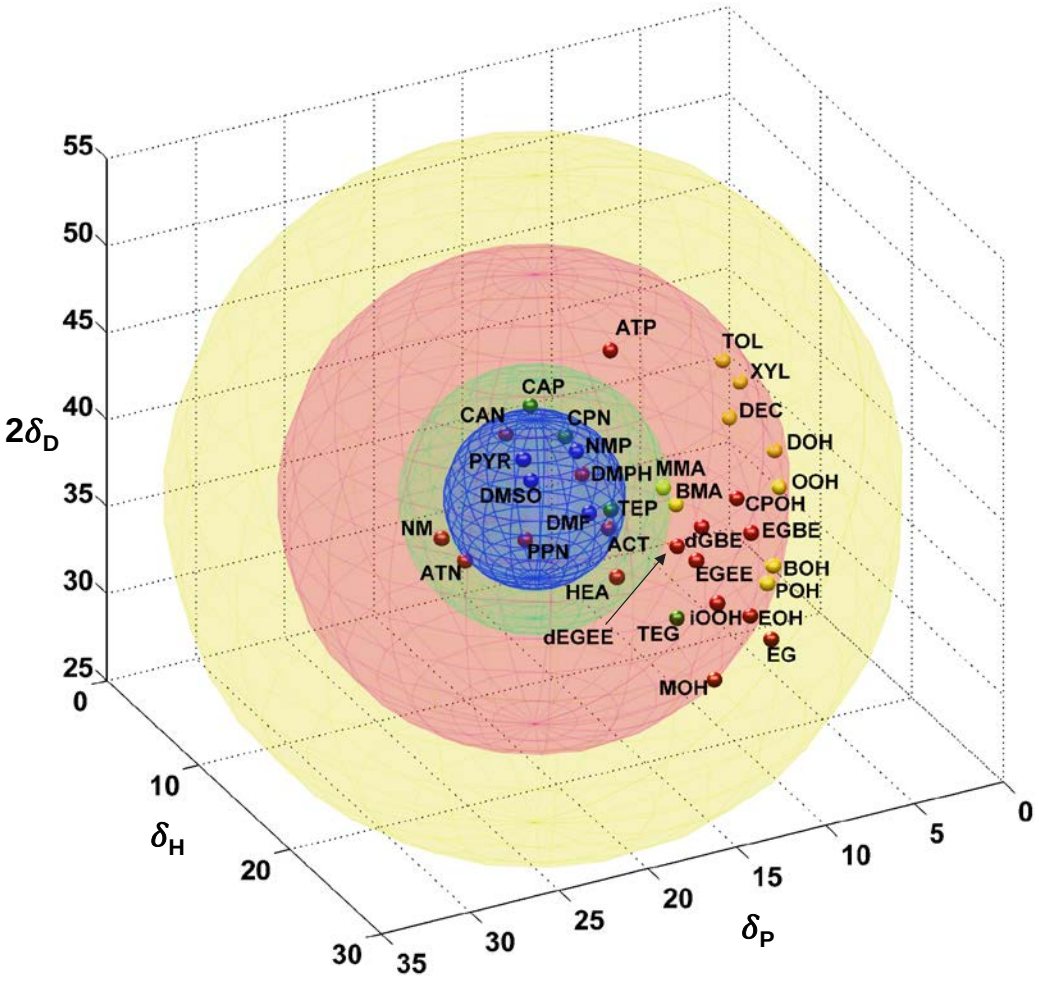

(b) 5% DBS

Sol (S) Center:

$(\delta_P, \delta_H, 2\delta_D)$ =

(15.7, 9.3, 35.1)

R_S = 4.6

R_{SG} = 6.9

R_{IG} = 12.9

R_I = 18.6

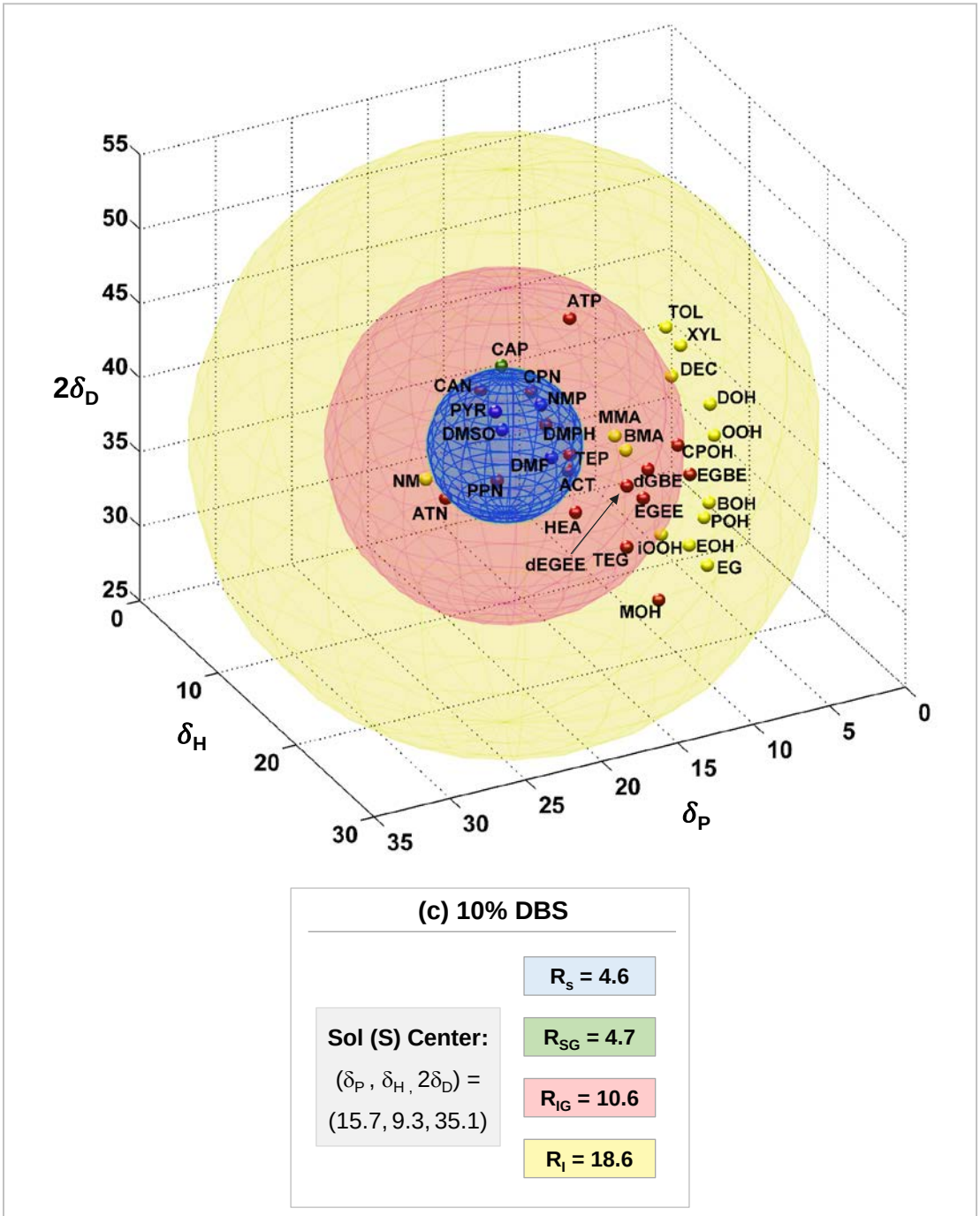

Figure 3.3. Results for DBS in various solvents, plotted in 3-D Hansen space: (a) 1%; (b) 5%; and (c) 10% DBS. The axes represent the three Hansen solubility parameters (δ_D = dispersive, δ_P = polar, and δ_H = hydrogen-bonding interactions). Each solvent is represented as a color-coded point on these plots. The results show a pattern of concentric spheres, i.e., the central sol (**S**) sphere in blue, followed in order by spheres corresponding to slow gel (**SG**) in green, instant gel (**IG**) in red, and insoluble (**I**) in yellow. The co-ordinates for the center of the **S** sphere and the radii of each sphere are indicated.

The plots in Figure 3.3 clearly reveal the key result mentioned above, which is the presence of a central solubility (**S**) sphere in blue followed by radiating spherical shells corresponding to **SG** (green), **IG** (red) and **I** (yellow) regions. The concentric spheres reflect our analysis procedure, but it is derived from the empirical observations. To emphasize this aspect, we show the empirical outcomes in the various solvents as discrete color-coded points. Note that the blue points are clustered in the center of the blue (**S**) sphere and as one moves radially outward, a number of green (**SG**) points appear, then several red (**IG**) points and finally some yellow (**I**) points. (As an aside, viewing the 3-D plots in 2-D can sometimes be misleading; i.e., points that appear to be inside a given sphere may actually be outside it.) There is uncertainty in the fitting of these spheres from the fact that solvent HSPs provided by Hansen are not exact values, from our fitting method, and from experimental error. It was found that this error does not take away from the trends observed. For example, the solubility 5% DBS sample shows a greater than a 0.95 goodness of fit within ±0.2 $MPa^{1/2}$ (thus R_S = 4.4-4.8). However, the underlying result in terms of a progression in Hansen space from solubility to gel to insoluble is in accord with the seminal paper by Raynal and Bouteiller,[16] although they did not separate out the **SG** and **IG** regions.

Several trends are evident from the plots in Figure 3.3. First, note that the blue sol (**S**) sphere is relatively large at 1% DBS (Figure 3.3a) and then shrinks to a constant size as the DBS concentration is increased to 5 and 10% (Figures 3.3b, 3.3c). This result reveals the concentration-dependent nature of molecular gelation: i.e., samples that are sols at low gelator concentrations may become gels at higher

gelator concentrations. Note also that the origin of the **S** sphere in the three above plots has a nearly constant location. The co-ordinates of the origin in terms of HSPs (δ_{D°, δ_{P°, δ_{H°) are (17.8, 13.6, 6.4) for 1% DBS, (17.6, 15.7, 9.3) for 5% DBS and (17.6, 15.7, 9.3) for 10% DBS (all numbers have units of $MPa^{½}$). The origin of the **S** sphere is significant because it provides an estimate for the HSPs of DBS itself. Interestingly, however, the above estimates are quite different from a recent calculation of the HSPs of DBS by a group contribution method, which determined (δ_{D°, δ_{P°, δ_{H°) to be (15.9, 3.9, 18.3) (again in $MPa^{½}$).[21] We believe this discrepancy indicates the difficulty of using group contribution methods to calculate HSPs for complex molecules. Note that the HSPs of DBS are expected to be close to those of the solvents in which it is most soluble. Empirically, we find that DBS is highly soluble (even at 10%) in polar aprotic solvents such as n-methylpyrrolidone (NMP), dimethylsulfoxide (DMSO), and dimethylformamide (DMF). All these solvents fall near the center of the **S** sphere and in turn, their HSPs are close to the values for the origin.

Next, we discuss trends in the **SG**, **IG** and **I** regions. At a low concentration (1%) of DBS, many gels form slowly after cooling and therefore the green **SG** region is large. Correspondingly, only few solvents reveal a gel as soon as the sample is cooled, and thus the red **IG** region is just a thin shell. As DBS is increased to 5%, the **SG** region shrinks while the **IG** region substantially expands. Finally, at 10% DBS, the **SG** region is a very thin, almost non-existent shell surrounding the **S** sphere and most of the gels are instant gels, i.e., fall in the **IG** region. In other words, when the conentration of gelator is high, gels rapidly form regardless of

solvent. Note also that the boundary of the **IG** region, i.e., the radius R_{IG} of the sphere, shrinks with increasing DBS. This means that some solvents are unable to completely solubilize high concentrations of DBS, which leads to a classification of these samples as insoluble (**I**). In turn, the **I** region expands with increasing DBS.

We will now mention a few trends regarding the chemical nature of the solvents tested and its impact on DBS gelation. As mentioned, DBS is highly soluble and non-gelling in polar aprotic solvents like NMP[25] and DMF. Conversely, in non-polar aliphatic liquids like n-alkanes, DBS is insoluble, as noted by previous studies.[21] DBS forms strong, instant gels even at low concentrations in aromatic solvents such as toluene and xylene, as well as in short-chain alcohols like propanol and butanol. In diols such as ethylene glycol as well as in glycol ethers, DBS shows slow gelation at low concentration and instant gelation at higher concentrations. Based on these findings, DBS gelation appears to be a complex process mediated by several weak interactions, which may include van der Waals, H-bonding, and possibly π-π stacking.[29] One cannot attribute the gelation ability of DBS simply to H-bonding[26] even though the molecule has two primary –OH groups. Indeed, DBS is able to gel solvents like the diols, which also have –OH groups that can compete for H-bonding.

3.3.4 SIGNIFICANCE OF THE S-SG-IG-I CONCENTRIC SHELLS

The 3-D plots for DBS shown in Figure 3.3 and illustrated in Figure 3.2 provide a logical framework for gelation. Researchers have recognized that gelation requires a balance between solubility and insolubility.[1-3] If a gelator is too soluble in a

solvent, i.e., if it is too similar or compatible with the solvent, it forms a sol. The HSPs allow us to quantify this intermolecular similarity. That is, if the HSPs of the gelator and the solvent are very close, then the mixture will fall in the solubility (**S**) sphere and will correspond to a sol.[16, 19] On the other extreme, if the gelator and solvent are too incompatible, i.e., if their HSPs are widely different, the gelator will be insoluble and the sample will fall in the **I** region. The incompatibility between solvent and gelator is proportional to the distance R_0 in 3-D space from the solvent point to the origin of the **S** sphere.[17] When R_0 is small such that $R_0 < R_S$, it corresponds to the soluble (**S**) region and when R_0 is large such that $R_0 > R_{IG}$, it corresponds to the **I** region. Note that R_0 can be calculated for a given solvent j (of known HSPs) if we know the HSPs at the origin of the S sphere:[17]

$$R_0 = \sqrt{4\left(\delta_D^j - \delta_{D^\circ}\right)^2 + \left(\delta_P^j - \delta_{P^\circ}\right)^2 + \left(\delta_H^j - \delta_{H^\circ}\right)^2} \qquad (3.2)$$

Between the above extremes, if the gelator is in a solvent that is moderately incompatible ($R_S < R_0 < R_{IG}$) then it forms a gel. Moreover, if the HSPs of the solvent are such that it falls just outside the sol (**S**) sphere, i.e., if $R_S \approx R_0$, then the gelator forms a slow gel (**SG**) in this solvent, at least at low gelator concentrations. On the other hand, if the HSPs of the solvent place it far from the **S** sphere and close to the **I** boundary (i.e., if $R_S << R_0 \approx R_{IG}$, the gelator forms an instant gel (**IG**) in this solvent even at low concentrations. There is a continuum between the **SG** and **IG** regions: increasing the gelator concentration causes the **SG** region to shrink and the **IG** region to expand. Conversely, the reverse (expansion of **SG**, shrinking of **IG**) is expected on increasing temperature.

3.3.5 GEL PROPERTIES AS A FUNCTION OF R_0

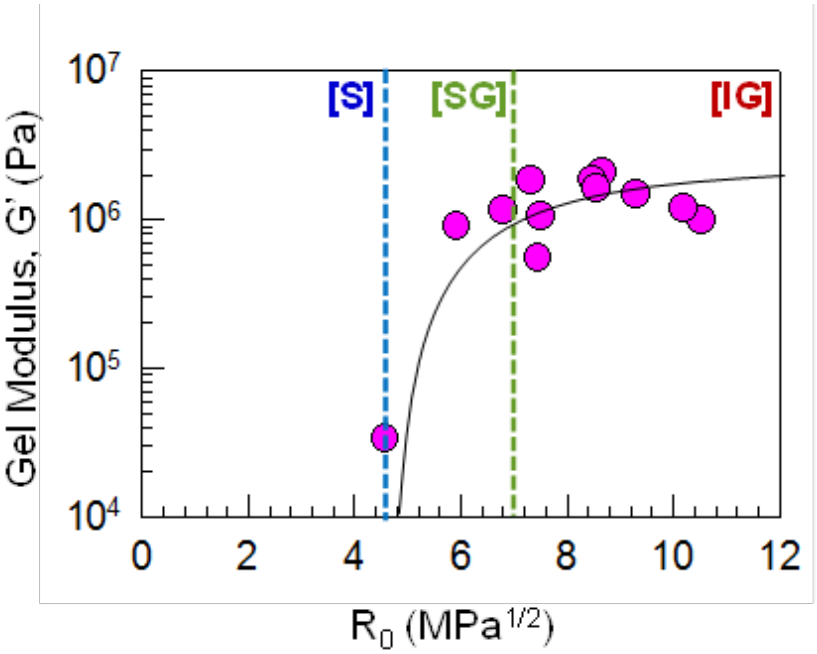

Figure 3.4. Correlation of gel modulus with Hansen parameters. The elastic modulus *G'* of 5% DBS gels in various solvents is plotted as a function of the distance R_0 of the corresponding solvent from the center of the solubility (**S**) sphere in Figure 3.3b. The values of R_0 at the boundaries of the **S** and **SG** regions are shown for reference. The data reveal an increasing trend in G' with R_0. The line is drawn to guide the eye.

The above analysis implies a systematic variation in gel properties with the distance R_0 from the center of the **S** sphere. That is, gels near the **S** boundary should take longer to form and should be weaker than those that are farther away from this boundary. To test these predictions, we have measured the elastic modulus G' from dynamic rheology for 5% DBS in a variety of solvents corresponding to the **SG** and **IG** regions. Figure 3.4 plots G' vs. the R_0 of the solvent. Note that the R_0 axis is on a linear scale while the G' axis is on a log scale. We confirmed that all the samples showed the signature of gels:[4, 33] i.e., in frequency sweeps, both the elastic modulus G' and the viscous modulus G''

were independent of frequency and G' exceeded G''. (In the case of the slow gels, we measured the rheology well after the gelation was complete.) For reference, the values of R_0 at the boundaries of the **S** and **SG** regions are indicated on Figure 3.4. The plot does show an increasing trend in gel modulus G' with increasing R_0 indicating that gels farther from the **S** boundary are stiffer. The trend is not perfect and many slow gels end up with moduli that are comparable to those of the instant gels. The one slow gel that lies closest to the **S** boundary has the lowest G'.

Next, we explored the relationship between gelation time t_{gel} and R_0, and this is presented in Figure 3.5. These measurements were done in various solvents corresponding to the **SG** and **IG** regions for 5% DBS. Again, note that the t_{gel} axis is on a log scale while the R_0 axis is on a linear scale. For representing the instant gels on a log scale, we have arbitrarily designated a low value of $t_{gel} = 10^{-1}$ min for them. The plot shows a decreasing trend in t_{gel} with increasing R_0 within the **SG** region. Again, this trend is not perfect and moreover, the distinction between slow and instant gel regions is not always clear-cut. Nevertheless, the limiting behavior is revealed by this plot. That is, at the edge of the soluble (**S**) region ($R_0 = 4.6$), $t_{gel} \rightarrow \infty$ as the favorable solvent-gelator interactions strongly interfere with the assembly of fibers. As the distance from the **S** region increases, t_{gel} decreases and at the other extreme, the plot levels out at $t_{gel} \rightarrow 0$ in the **IG** region.

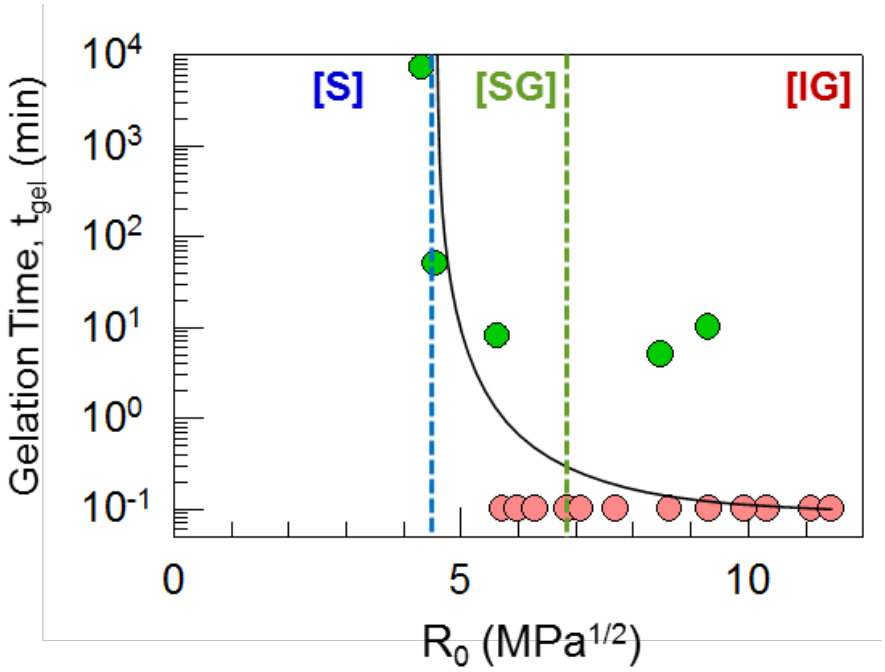

Figure 3.5. Correlation of gelation time with Hansen parameters. For the case of 5% DBS gels in various solvents, the time to form a gel after cooling to room temperature (t_{gel}) is plotted as a function of the distance R_0 of the corresponding solvent from the center of the solubility (**S**) sphere in Figure 3.3b. For each of the instant gel (**IG**) points (red circles), a gelation time of 10^{-1} min is arbitrarily assigned. The slow gel (**SG**) points are shown as green circles. Note that some **SG** points occur in the **IG** region and vice versa; this is unavoidable with the fitting algorithm employed. The values of R_0 at the boundaries of the **S** and **SG** regions are shown for reference. At the boundary of the **S** region, t_{gel} diverges. As one moves away from this boundary, t_{gel} tends to decrease with increasing R_0. The curve is drawn to guide the eye.

3.3.6 Prediction of Gelator Behavior in Solvent Mixtures

Based on the above analysis, we can offer a few predictions and put them to the test. For example, consider mixtures of two miscible solvents with known HSPs. The HSPs of the mixtures can be estimated by linear interpolation based on the HSPs of the pure solvents and their volume fractions (assuming ideal mixing).[17] On the 3-D plot, this corresponds to straight lines between the two solvent points. Can we predict the

outcomes for the gelator DBS in such mixtures based on the locations of the points on the 3-D plot?

To test this, we have considered DMSO as one of the solvents. DBS is highly soluble in DMSO and thus this solvent point occurs in the middle of the **S** region (Figure 3.6). We then considered five solvents: three fatty alcohols (decanol, octanol, and butanol), toluene, and ethylene glycol. These solvents fall in the **I** or **IG** regions. We examined 5% DBS in blends of DMSO with these five solvents. The points corresponding to these mixtures fall along five lines on the 3-D plot, as shown in Figure 3.6, and the color-coded empirical outcomes for each of these mixtures is indicated. For each solvent pair, we see a progression from solubility (blue points) in DMSO to slow gel (green points) to instant gel (red points). For the three alcohols and toluene, insolubility (yellow points) are seen at high alcohol fractions. Note that the blue points fall a bit outside the solubility (**S**) sphere determined previously for neat solvents; however, the correct trend is seen in all cases. The differences may arise due to non-ideal mixing of the solvents.

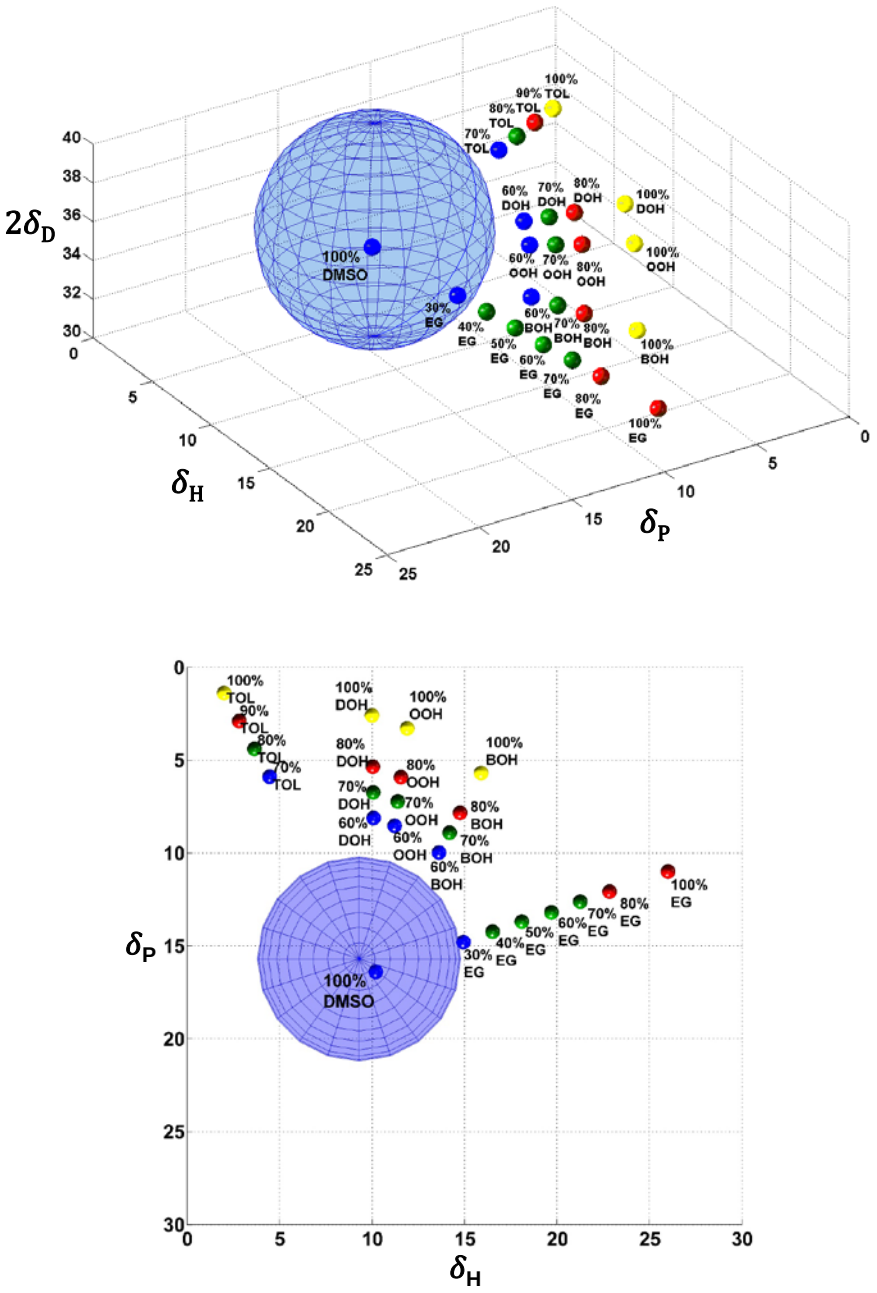

Figure 3.6. Outcomes for DBS in solvent blends, plotted in 3-D Hansen space: side view (top) and overhead view (bottom). DBS was studied at a concentration of 5% in mixtures of DMSO and the following solvents: toluene (TOL), 1-decanol (DOH), 1-octanol (OOH), 1-butanol (BOH) and ethylene glycol (EG). On the Hansen plot, solvent mixtures fall on straight lines between the points corresponding to the individual solvents. DBS is highly soluble in DMSO, and the pure DMSO point is near the center of the solubility (**S**) sphere. For the mixtures, the sample outcomes are color coded as: sols (**S**, blue), slow gels (**SG**, green), instant gels (**IG**, red) and insoluble (**I**, yellow). A systematic progression in sample outcomes is seen for all the solvent pairs.

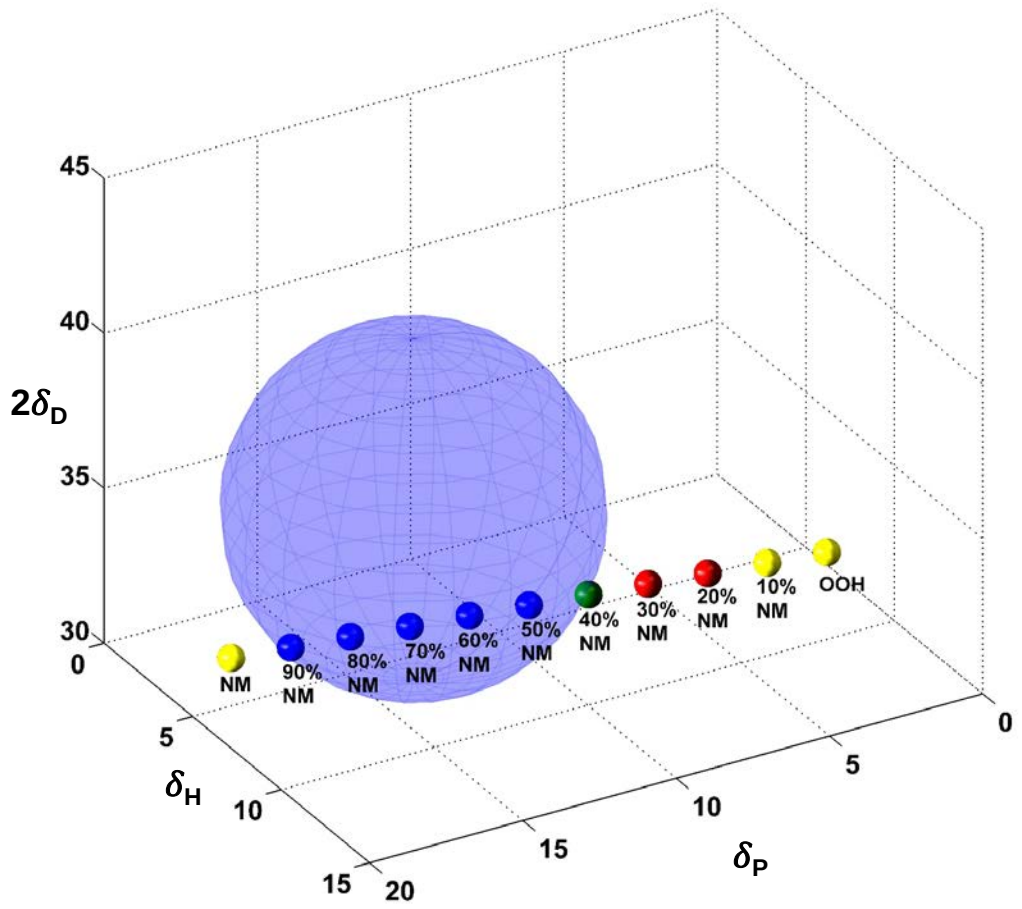

Figure 3.7. Predicted behavior of DBS in blends of two solvents in which it is insoluble. As an example, for the case of 10% DBS, we consider nitromethane (NM) and 1-octanol (OOH) as two solvents in which it is insoluble. As seen above, the two solvents occur on either side of the solubility (S) sphere. Thus, a line drawn between the solvents is expected to pass through all the 4 regions, i.e., sol (**S**, blue), slow gels (**SG**, green), instant gels (**IG**, red) and insoluble (**I**, yellow), depending on the ratios of the solvents.

We conclude from Figure 3.6 that our analysis based on HSPs has reasonably good predictive power. That is, for a given gelator, once the center of the **S** sphere and the sizes of the **S**, **SG** and **IG** spheres are determined, we can predict to a first approximation the behavior of the gelator in a new solvent (with unknown identity) based only on the solvent's HSP values.[22, 23] One application of this approach has been reported recently and it involved taking a gelator that was insoluble in two neat

solvents, but allowing it to form a gel in mixtures of these two solvents.[23] Similarly, for the present study, we apply similar logic behind such an experimental outcome to predict the behavior of DBS in nitromethane and octanol solvent mixtures in Figure 3.7. If the gelator is insoluble (I) in two solvents that fall on either side of the solubility (S) sphere, then a line drawn between the two solvents cuts through the S, SG and IG regions. For example, two such solvents in the case of DBS are nitromethane and 1-octanol. Depending on the ratio of these two solvents, DBS samples are predicted to range from sols to slow gels to instant gels, as shown by Figure 3.7.

3.3.7 THUMB RULES AND OUTLOOK

In terms of thumb rules (independent of concentration) for the distance R_0 from the center of the **S** sphere, we estimate that $R_0 < 5$ MPa^{½} results in solubility; $R_0 \sim 10$ MPa^{½} results in gelation; and $R_0 \sim 15$ MPa^{½} results in insolubility. It will be interesting to apply this analysis to other gelators and to test the validity of the above thumb rules. Note that all three HSPs need to be used to calculate R_0 by eq 1. That is, the difference in *total cohesive energy density* between gelator and solvent is what dictates gelation behavior.

To facilitate the application of our approach to other gelators, we have developed a **standalone program and graphical user interface** (based on underlying MATLAB code) and we will make this freely available on the Internet (upon request). Our program enables a user to input data for their gelator of interest in different solvents in the form of a Microsoft Excel spreadsheet. The spreadsheet has to adhere to a set template, which includes a list of solvents with their HSPs and the outcomes with the

gelator (sol, slow gel, instant gel, insoluble) for each case. The program then generates 3-D Hansen plots similar to those shown in Figure 3.3. Screenshots of the program were shown in Figure 3.1. Two modes of fitting are offered. In one mode, the user may fit the regions as shells radiating from a central solubility sphere, as was done in Figure 3.3. In the other mode, the user may fit the regions as discrete spheres in Hansen space. The program calculates the centers and radii of the spheres corresponding to optimal goodness-of-fit values. Our method enables simple benchtop data on gelators to be visualized and analyzed for insights.

3.4. CONCLUSIONS

We have applied a simple methodology to systematically characterize the behavior of the model organogelator DBS in a number of organic solvents. We visually classified gelator behavior through benchtop experiments and plotted the various outcomes on 3-D plots where the axes correspond to the three Hansen solubility parameters (HSPs). The results follow a pattern of concentric spheres with a central solubility (**S**) sphere surrounded by spherical regions corresponding to slow gelation (**SG**), instant gelation (**IG**), and insolubility (**I**). The pattern suggests that gelation requires a moderate extent of incompatibility between the gelator and solvent. The latter can be quantified by the distance R_0 from the center of the **S** sphere. The modulus of the organogels increases with R_0 while the time to form the gels decreases with R_0. Our approach gives reasonable predictions of gelator behavior in untested solvents, such as solvent blends. Some thumb rules based on the above approach have been developed for DBS for prediction of behavior in untested solvents. We believe that similar thumb rules can be

established for other gelators via our approach. A MATLAB program and an associated graphical user interface (GUI) have been developed to allow other researchers to apply the same approach to their gelators.

Chapter 4: CONCLUSIONS & FUTURE DIRECTIONS

4.1. CONCLUSIONS

In this thesis, we have presented a simple framework for understanding the self-assembly outcomes of a model organogelator DBS in various solvents at three concentrations. We observed four distinct outcomes from the addition of DBS to a given sample: soluble, slow gel, instant gel, insoluble. Each sample outcome was plotted in three-dimensional Hansen space according to the solvent's Hansen parameter and the sample outcome. Spheres were fit to the regions of DBS behavior via an algorithm in MATLAB and it was found that concentric spheres of slow gel, instant gel, and insoluble regions radiating out from the central solubility sphere provided a good fit. Likewise, DBS behavior in mixtures of solvents of a good solvent (solubilizes DBS) and a bad solvent (DBS is insoluble) were observed and plotted. For these solvent mixtures, the regions of solubility were generally larger than those of the neat solvents. Still, for each solvent mixture, a transition through the expected regions of soluble, slow gel, instant gel, and insoluble was observed.

4.2. FUTURE DIRECTIONS

The work presented in this thesis lays the groundwork for future studies to gain deeper insights into the principles behind organogelation for DBS and for all other gelators. As mentioned, in the process of our analysis, we have developed an algorithm coded in MATLAB and an easy-to-use graphical user interface (GUI) that will be made

available to the scientific community at no cost upon request. It is our hope that this software will enable our lab and others to tackle some significant questions that remain in the field. Three such questions are indicated below.

1. Does the pattern of concentric shells of sample outcomes moving from solubility to gelation to insolubility hold for other gelators or is this phenomenon unique to DBS? In our study, we chose DBS as a model organogelator because of its well-known ability to gel many different types of solvents and our previous familiarity with it. The trends seen in our 3D Hansen plots are surprisingly accurate and elegant. Indeed this sort of behavior has not been shown in the literature studies around HSPs and gelators. However, this model for gelator behavior does make intuitive sense. One possibility is that the reliance of DBS on two-types of weak bonding (hydrogen bonding and bonds) may introduce a strong dependence on δ_P, and δ_H in Hansen space. On the contrary, a gelator that relies solely on hydrogen bonding may show a much stronger dependence on δ_H than on δ_P. It will be interesting to see if the concentric shell model holds for other types of gelators and could significantly boost the community's understanding of the mechanisms underlying various gelators.

2. What are the effects of various functional substituents on the 3D Hansen plot DBS? Can we learn to tune a molecule such as DBS to gel specific solvents with simple chemical modifications? In this work we have establish clear boundaries to the behavior of DBS in various solvents at three different concentrations. In the future, it might be interesting to re-test the same solvents on a DBS-derivative with various

functional substituents, such as (electron-donating, electron-accepting, bulky steric, etc.). It is possible that by adding groups we may be able shift the DBS regions to achieve gelation in a solvent which was previously soluble or insoluble. This method of testing substituents and applying our mapping method to chart the gelator behavior also provides a systematic means of determining the function of substituent groups. Likewise, the same method may be applied to other existing molecular gelators. First, the preliminary behavior of the native molecule can be characterized by our method. Then by substituting new functional groups onto the molecule, a researcher can potentially tune the behavior of the gelator to achieve gels in solvents for which the molecule was initially non-gelling.

3. Can we draw understanding into the mixture behaviors that lead to shift in the solubility and gelation regions from the neat solvent Hansen plots to the DMSO mixture Hansen plots? In our study, we have generated 3D Hansen plots for our gelator in both a collection of neat solvents and in mixtures of solvents in which DBS is typically soluble and non-soluble. In comparing these plots, it is noted that there is a shift in the sample outcome boundaries between the two plots. For example, in the DMSO blends, the solubility sphere is greatly expanded compared to the neat solvent data. However, the same trend in sample behavior, moving from soluble to slow gel to instant gel to insoluble remains for all solvent mixtures studied. While we have not been able to draw a full understanding of the complexities of gelation of solvent mixtures, our study represents a promising step toward gaining clarity. In the future, studies on the mixture properties governing these systems would be of great interest.

This knowledge would eventually enable the design of gelator systems with controlled gelation kinetics, with controlled elastic modulus and without harmful solvents. Each of these properties could be tuned to the final application of the molecular gel, thus unlocking the potential of these fascinating molecules.

References

1. Weiss, R. G.; Terech, P., *Molecular Gels: Materials with Self-Assembled Fibrillar Networks*. Springer: Dordrecht, 2006.

2. Terech, P.; Weiss, R. G., Low molecular mass gelators of organic liquids and the properties of their gels. *Chemical Reviews* **1997,** 97, (8), 3133-3159.

3. Sangeetha, N. M.; Maitra, U., Supramolecular gels: Functions and uses. *Chemical Society Reviews* **2005,** 34, (10), 821-836.

4. Raghavan, S. R.; Douglas, J. F., The conundrum of gel formation by molecular nanofibers, wormlike micelles, and filamentous proteins: gelation without cross-links? *Soft Matter* **2012,** 8, (33), 8539-8546.

5. Jadhav, S. R.; Vemula, P. K.; Kumar, R.; Raghavan, S. R.; John, G., Sugar-derived phase-selective molecular gelators as model solidifiers for oil spills. *Angewandte Chemie-International Edition* **2010,** 49, (42), 7695-7698.

6. Carretti, E.; Bonini, M.; Dei, L.; Berrie, B. H.; Angelova, L. V.; Baglioni, P.; Weiss, R. G., New frontiers in materials science for art conservation: Responsive gels and beyond. *Accounts of Chemical Research* **2010,** 43, (6), 751-760.

7. Sun, K. S.; Oh, H.; Emerson, J. F.; Raghavan, S. R., A new method for centrifugal separation of blood components: Creating a rigid barrier between density-stratified layers using a UV-curable thixotropic gel. *Journal of Materials Chemistry* **2012,** 22, (6), 2378-2382.

8. Basrur, V. R.; Guo, J. C.; Wang, C. S.; Raghavan, S. R., Synergistic gelation of silica nanoparticles and a sorbitol-based molecular gelator to yield highly-conductive free-standing gel electrolytes. *Acs Applied Materials & Interfaces* **2013,** 5, (2), 262-267.

9. Dastidar, P., Supramolecular gelling agents: Can they be designed? *Chemical Society Reviews* **2008,** 37, (12), 2699-2715.

10. Dawn, A.; Shiraki, T.; Haraguchi, S.; Tamaru, S.; Shinkai, S., What kind of "soft materials" can we design from molecular gels? *Chemistry-an Asian Journal* **2011,** 6, (2), 266-282.

11. Hirst, A. R.; Smith, D. K., Solvent effects on supramolecular gel-phase materials: Two-component dendritic gel. *Langmuir* **2004,** 20, (25), 10851-10857.

12. Hirst, A. R.; Coates, I. A.; Boucheteau, T. R.; Miravet, J. F.; Escuder, B.; Castelletto, V.; Hamley, I. W.; Smith, D. K., Low-molecular-weight gelators: Elucidating the principles of gelation based on gelator solubility and a cooperative

self-assembly model. *Journal of the American Chemical Society* **2008,** 130, (28), 9113-9121.

13. Edwards, W.; Lagadec, C. A.; Smith, D. K., Solvent-gelator interactions-using empirical solvent parameters to better understand the self-assembly of gel-phase materials. *Soft Matter* **2011,** 7, (1), 110-117.

14. Chen, J.; Kampf, J. W.; McNeil, A. J., Comparing molecular gelators and nongelators based on solubilities and solid-state interactions. *Langmuir* **2010,** 26, (16), 13076-13080.

15. Muro-Small, M. L.; Chen, J.; McNeil, A. J., Dissolution Parameters Reveal Role of Structure and Solvent in Molecular Gelation. *Langmuir* **2011,** 27, (21), 13248-13253.

16. Raynal, M.; Bouteiller, L., Organogel formation rationalized by Hansen solubility parameters. *Chemical Communications* **2011,** 47, (29), 8271-8273.

17. Hansen, C. M., *Hansen Solubility Parameters: A User's Handbook*. CRC Press: Boca Raton, Fla., 2000; p 208 p.

18. Hansen, C. M., 50 Years with solubility parameters - past and future. *Progress in Organic Coatings* **2004,** 51, (1), 77-84.

19. Gao, J.; Wu, S.; Rogers, M. A., Harnessing Hansen solubility parameters to predict organogel formation. *Journal of Materials Chemistry* **2012,** 22, (25), 12651-12658.

20. Xu, H. Q.; Song, J.; Tian, T.; Feng, R. X., Estimation of organogel formation and influence of solvent viscosity and molecular size on gel properties and aggregate structures. *Soft Matter* **2012,** 8, (12), 3478-3486.

21. Liu, S. J.; Yu, W.; Zhou, C. X., Solvents effects in the formation and viscoelasticity of DBS organogels. *Soft Matter* **2013,** 9, (3), 864-874.

22. Yan, N.; Xu, Z. Y.; Diehn, K. K.; Raghavan, S. R.; Fang, Y.; Weiss, R. G., Pyrenyl-Linker-Glucono Gelators. Correlations of Gel Properties with Gelator Structures and Characterization of Solvent Effects. *Langmuir* **2013,** 29, (2), 793-805.

23. Yan, N.; Xu, Z.; Diehn, K. K.; Raghavan, S. R.; Fang, Y.; Weiss, R. G., How do liquid mixtures solubilize insoluble gelators? Self-assembly properties of pyrenyl-linker-glucono gelators in tetrahydrofuran-water mixtures. *Journal of the American Chemical Society* **2013,** 135, 8989-8999

24. Yamasaki, S.; Tsutsumi, H., Microscopic studies of 1,3-2,4-di-O-benzylidene-D-sorbitol in ethylene glycol. *Bulletin of the Chemical Society of Japan* **1994,** 67, (4), 906-911.

25. Smith, J. M.; Katsoulis, D. E., Gelation of Silicone Fluids Using 1,3/2,4-Dibenzylidene Sorbitol. *Journal of Materials Chemistry* **1995,** 5, (11), 1899-1903.

26. Yamasaki, S.; Tsutsumi, H., The Dependence of the Polarity of Solvents on 1,3/2,4-Di-O-Benzylidene-D-Sorbitol Gel. *Bulletin of the Chemical Society of Japan* **1995,** 68, (1), 123-127.

27. Mercurio, D. J.; Khan, S. A.; Spontak, R. J., Dynamic rheological behavior of DBS-induced poly(propylene glycol) physical gels. *Rheologica Acta* **2001,** 40, (1), 30-38.

28. Frassdorf, W.; Fahrlander, M.; Fuchs, K.; Friedrich, C., Thermorheological properties of self-assembled dibenzylidene sorbitol structures in various polymer matrices: Determination and prediction of characteristic temperatures. *Journal of Rheology* **2003,** 47, (6), 1445-1454.

29. Wilder, E. A.; Hall, C. K.; Khan, S. A.; Spontak, R. J., Effects of composition and matrix polarity on network development in organogels of poly(ethylene glycol) and dibenzylidene sorbitol. *Langmuir* **2003,** 19, (15), 6004-6013.

30. Dumitras, M.; Friedrich, C., Network formation and elasticity evolution in dibenzylidene sorbitol/poly(propylene oxide) physical gels. *Journal of Rheology* **2004,** 48, (5), 1135-1146.

31. VanderHart, D. L.; Douglas, J. F.; Hudson, S. D.; Antonucci, J. M.; Wilder, E. A., NMR Characterization of the Formation Kinetics and Structure of Di-O-Benzylidene Sorbitol Gels Self-Assembled in Organic Solvents. *Langmuir* **2011,** 27, (5), 1745-1757.

32. Schamper, T.; Jablon, M.; Randhawa, M. H.; Senatore, A.; Warren, J. D., Acid Stable Dibenzylidene Sorbitol Gelled Clear Solid Antiperspirant Formulations .1. *Journal of the Society of Cosmetic Chemists* **1986,** 37, (4), 225-231.

33. Raghavan, S. R.; Cipriano, B. H., Gel formation: Phase diagrams using tabletop rheology and calorimetry. In *Molecular Gels*, Weiss, R. G.; Terech, P., Eds. Springer: Dordrecht, 2005; pp 233-244.

34. Huang, X.; Terech, P.; Raghavan, S. R.; Weiss, R. G., Kinetics of 5 alpha-cholestan-3 beta,6-yl N-(2-naphthyl)carbamate/n-alkane organogel formation and its influence on the fibrillar networks. *Journal of the American Chemical Society* **2005,** 127, (12), 4336-4344.